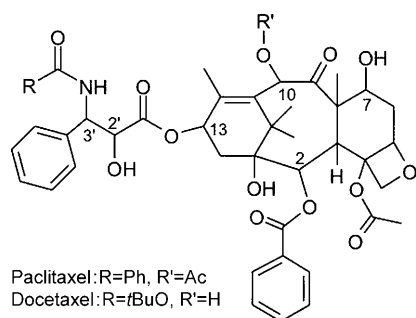


## Differences in Paclitaxel and Docetaxel Interactions with Tubulin Detected by Mutagenesis of Yeast Tubulin

Robert D. Winefield,<sup>[a]</sup> Ruth A. Entwistle,<sup>[a]</sup> Travis B. Foland,<sup>[a]</sup> Gerald H. Lushington,<sup>[b]</sup> and Richard H. Himes<sup>\*,[a]</sup>

Paclitaxel and a semi-synthetic analogue docetaxel are two taxane antitumor agents that are used against a number of cancers.<sup>[1]</sup> The taxanes bind to the  $\beta$ -subunit of the dimeric



protein  $\alpha,\beta$ -tubulin in microtubules in a 1:1 molar ratio, resulting in a decrease in the dynamic nature of microtubules leading to mitotic arrest and apoptotic cell death.<sup>[2]</sup> The taxanes also promote the assembly of tubulin into microtubules.<sup>[3]</sup> Docetaxel is two to three times as effective as paclitaxel in promoting the assembly of mammalian brain tubulin in vitro, and has a binding constant that is greater than that of paclitaxel by the same factor.<sup>[4]</sup> We have been using site-directed mutagenesis of *Saccharomyces cerevisiae*  $\beta$ -tubulin to examine the taxane binding site in tubulin. Although wild-type *S. cerevisiae* tubulin does not bind taxanes, we were able to instill taxane binding by making five mutations in  $\beta$ -tubulin.<sup>[5]</sup> The rationale for choosing the five sites to mutate was based on the electron crystal structure of the mammalian brain tubulin–paclitaxel complex.<sup>[6]</sup> This structure indicated that the amino acid side chains, Lys 19, Val 23, Asp 26, His 227 and Phe 270, are important in taxane binding. In *S. cerevisiae*  $\beta$ -tubulin these sites are occupied by different amino acids, Ala 19, Thr 23, Gly 26, Asn 227, and Tyr 270. When we exchanged the five residues for those that occur in brain  $\beta$ -tubulin, yeast tubulin was able to bind paclitaxel.<sup>[5]</sup> We are currently in the process of determining the relative importance of each residue to taxane binding by systematically reversing our original mutations. As a screen to measure the effects of the changes, we are using a cell-based assay in which we examine effects of the mutations on cell proliferation. To enable the use of a cell-based assay, we introduced the mutated  $\beta$ -tubulin gene into a yeast strain that has

diminished multidrug transport activity<sup>[7]</sup> to produce a strain that is sensitive to paclitaxel (AD1-8-tax).<sup>[8]</sup> In the course of these studies we found interesting differences in the sensitivity of the various strains to paclitaxel and docetaxel.

The effect of the two taxanes on the growth of the strains is presented in Table 1. The letters B and Y refer to the five resi-

**Table 1.** Growth inhibition by paclitaxel and docetaxel.

Strain	Paclitaxel <sup>[a]</sup> [%]	Paclitaxel <sup>[b]</sup> ID <sub>50</sub> [ $\mu$ M]	Docetaxel <sup>[a]</sup> [%]	Docetaxel <sup>[b]</sup> ID <sub>50</sub> [ $\mu$ M]
BBBBB	97	6.3 $\pm$ 0.3	100	4.5 $\pm$ 0.1
YYYYY	0	–	0	–
YBBBB	92	4.6 $\pm$ 0.4	67	22 $\pm$ 1.0
BYBBB	0	–	0	–
BBYBB	0	–	0	–
BBBYB	100	4.3 $\pm$ 0.2	37	26 $\pm$ 2.6
BBBBY	0	–	0	–

[a] Inhibition at a concentration of 25  $\mu$ M. [b] Standard deviations are shown.

dues found in brain and *S. cerevisiae* tubulin, respectively. The data show that 25  $\mu$ M of either taxane completely inhibited growth of the strain with brain  $\beta$ -tubulin residues at the five positions (BBBBB), but had no effect on the strain with yeast residues (YYYYY). When positions 23, 26, and 270 were changed back to the residues in yeast  $\beta$ -tubulin, the strains (BYBBB, BBYBB, BBBBY) were insensitive to both taxanes, indicating the importance of these residues to taxane binding. However, substituting a yeast residue at position 19 (YBBBB) or 227 (BBBYB) did not affect the sensitivity to paclitaxel, i.e., the paclitaxel ID<sub>50</sub> values were essentially unchanged. On the other hand, the sensitivity of these two strains to docetaxel decreased. The K19A and H227N mutations caused the ID<sub>50</sub> value for docetaxel to increase approximately five- to sixfold.

To further examine the effect of the H227N mutation, tubulin was purified from this strain (BBBYB) as well as from AD1-8-tax (BBBBB) and used in in vitro assembly and binding experiments. Data presented in Figure 1 demonstrate that assembly was dependent on the taxanes and that, in the case of tubulin from strain BBBBB (Figure 1a), the EC<sub>50</sub> values for paclitaxel and docetaxel were 1.1  $\mu$ M and 0.36  $\mu$ M, respectively. However, with tubulin from the H227N (BBBYB) strain, the values were 2.2  $\mu$ M for paclitaxel and 3.0  $\mu$ M for docetaxel (Figure 1b). Thus, the H227N mutation increased the ED<sub>50</sub> value for docetaxel 8.3-fold, but had a much less effect on the ED<sub>50</sub> value of paclitaxel (twofold increase). The formation of microtubules in these experiments was verified by electron microscopy (data not shown). The effect of the H227N mutation on the tubulin–docetaxel interaction was also seen in a competition-binding

[a] Dr. R. D. Winefield, Dr. R. A. Entwistle, T. B. Foland, Prof. R. H. Himes  
Department of Molecular Biosciences, University of Kansas  
Lawrence, Kansas 66045-7534 (USA)  
Fax: (+1) 785-864-5321  
E-mail: himes@ku.edu

[b] Dr. G. H. Lushington  
Molecular Graphics & Modeling Laboratory, University of Kansas  
Lawrence, Kansas 66045-7582 (USA)

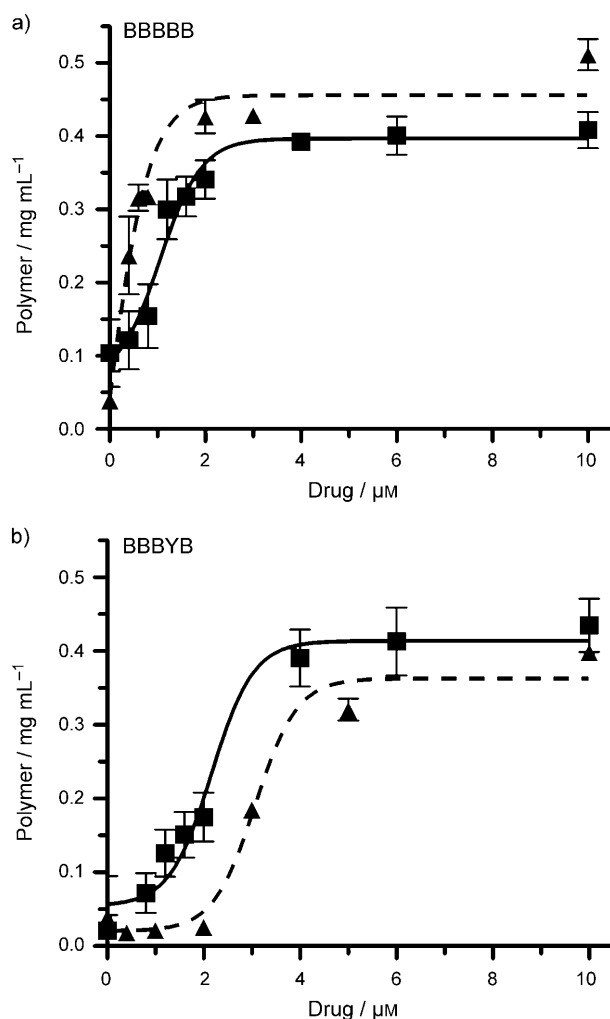


**Figure 1.** Effect of the H227N mutation on the assembly of yeast tubulin; a) strain BBBBB; b) strain BBBYB; paclitaxel ■, docetaxel ▲. Error bars refer to standard error of the mean.

assay. Preformed microtubules were incubated with 5 μM <sup>3</sup>H-paclitaxel and a varying concentration of docetaxel. The data in Figure 2 show that the H227N mutation decreased the inter-

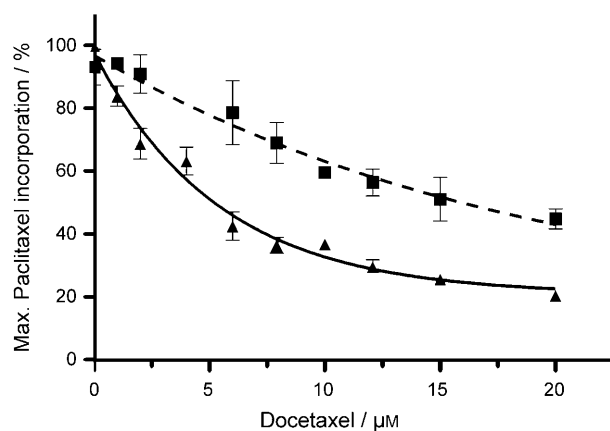


**Figure 2.** Effect of the H227N mutation on the displacement of <sup>3</sup>H-paclitaxel by docetaxel; BBBBB ▲, BBBYB ■.

action of docetaxel with yeast tubulin by a factor of three to four, i.e., a three to four times higher concentration of docetaxel was required to decrease paclitaxel binding by 50%.

To help explain the consequences of having Asn instead of His at residue 227 on paclitaxel and docetaxel activity, we modeled the T-taxol conformation of bound paclitaxel<sup>[6]</sup> into the binding sites of the two proteins. The T-taxol conformation appears to be the most widely accepted conformation for tubulin-bound paclitaxel<sup>[11–14]</sup>. We assumed that the basic conformers for paclitaxel and docetaxel would be largely conserved relative to the T-taxol structure reported in the 1 JFF crystal structure for both proteins, and thus constructed preliminary models for each of the four relevant complexes; paclitaxel-BBBBB, docetaxel-BBBBB, paclitaxel-BBBYB, and docetaxel-BBBYB, by simply editing the original crystal structure accordingly and effecting local receptor relaxation in the vicinity of the ligand.

From these computations, we derived a purely enthalpic estimate that docetaxel bound more strongly than paclitaxel to the BBBBB tubulin by 0.43 kcal mol<sup>-1</sup>, and that paclitaxel bound more strongly than docetaxel to the BBBYB tubulin by 1.94 kcal mol<sup>-1</sup>. The main source of the enthalpy difference in the BBBBB case is van der Waals interactions, which are derived from stronger interactions between the bulkier docetaxel *tert*-butyl group at the 3'-N position with His227 and Val23 than are achieved by the longer, less bulky phenyl group at this position on paclitaxel. In the case of the BBBYB tubulin, our calculations suggest that docetaxel may lose a significant portion of the van der Waals advantage relative to paclitaxel by virtue of the His to Asn mutation (Asn is less lipophilic). Paclitaxel, however, might gain a binding advantage to BBBYB tubulin by virtue of stronger H-bonding interaction between the benzamide carbonyl and the Asn227 side chain NH donor site (2.22 Å) than is possible for the carbamate carbonyl of docetaxel (2.48 Å) (Figure 3). The combined effects of the decreased van der Waals interaction of docetaxel and the increased H-bonding interaction of paclitaxel to BBBYB tubulin might thus result in stronger binding by paclitaxel.

In comparing the predicted binding conformers for paclitaxel and docetaxel with BBBBB and YBBBB, our calculations suggest that the hydrogen atoms on the C<sub>5</sub> of the Lys19 side chain approach within 4.0 Å of the *tert*-butyl group of docetaxel (a favorable distance from the perspective of van der Waals interactions) but that no Lys19 atom comes within 6.1 Å of any atom on the corresponding paclitaxel benzamide ring. Mutation of Lys to a smaller Ala residue might thus remove a favorable lipophilic contact from docetaxel, but suggests very minimal effect on paclitaxel binding.

In summary, we have shown that the relative effects of paclitaxel and docetaxel on tubulin can be affected differently by mutations in β-tubulin. The yeast tubulin mutagenesis approach that we have developed is a useful tool in the development of new taxane and other microtubule antimetabolic agents.

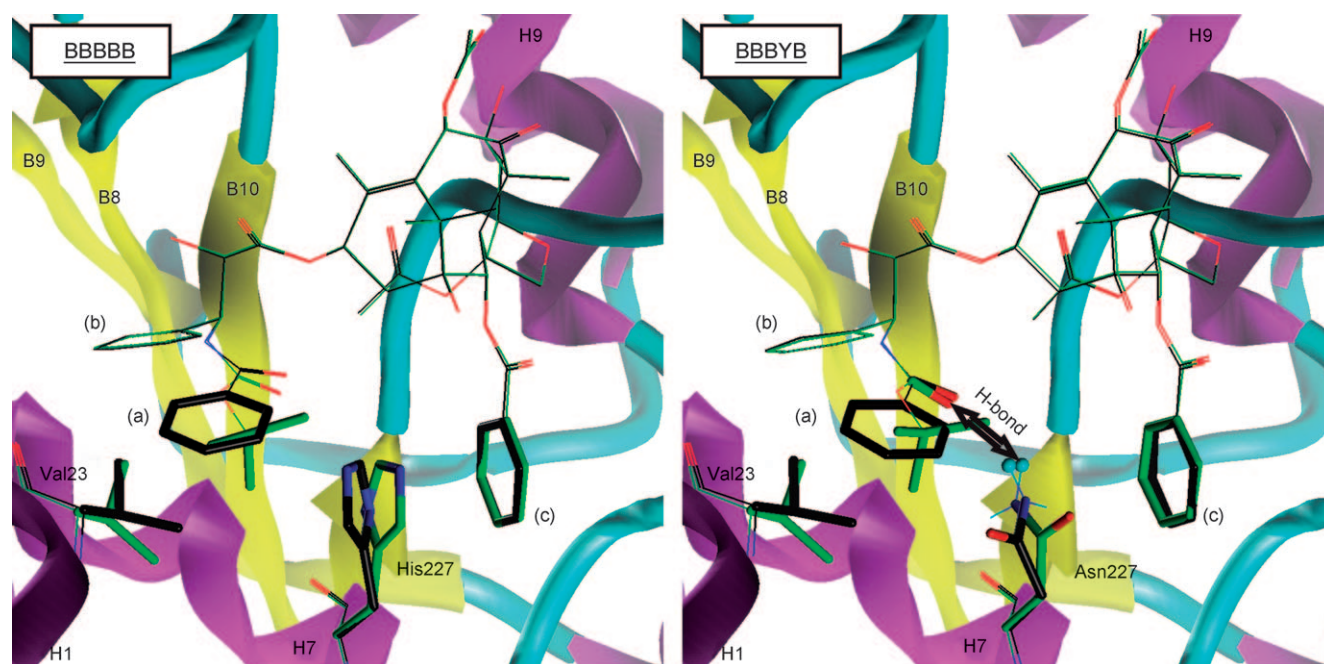


**Figure 3.** Molecular model showing the His227 and Asn227 residues in the tubulin–paclitaxel and tubulin–docetaxel complexes. The position of paclitaxel and interacting residues are shown (black) superimposed over docetaxel and interacting residues (green). Helices (purple),  $\beta$ -strands (yellow), and loops (light blue), are shown along with oxygen (red), nitrogen (dark blue), and hydrogen atoms (light blue spheres). Helices and  $\beta$ -strands are labeled sequentially according to the  $\beta$ -tubulin sequence along with the C-3' benzamido (a), the C-3' phenyl (b), and the C2-benzoyl phenyl groups (c) belonging to paclitaxel and docetaxel. In the BBBYB complexes formation of an H-bond between the Asn227 side chain and the carbonyl oxygen of the paclitaxel benzamido and the docetaxel carbamate groups is shown.

## Experimental Section

**Tubulin mutations and purification:** Mutations were introduced into the single  $\beta$ -tubulin gene (TUB2) of the *S. cerevisiae* strain AD 12345678 (AD1-8)<sup>[7]</sup> using procedures described previously.<sup>[8]</sup> Thus, wild-type  $\beta$ -tubulin is not produced by the mutant strains.  $\beta$ -Tubulin in these strains also carries a His<sub>6</sub> tag at the C-terminus. His<sub>6</sub>-tagged tubulin was purified using a previously developed immobilized metal chelating chromatography procedure.<sup>[5]</sup>

**Yeast proliferation assay:** The cell proliferation assays were conducted in triplicate in 96-well plates containing 2,000 cells per well in YPD-media (2% glucose, 1% yeast extract, and 2% peptone) supplemented with penicillin (100 U/mL) and streptomycin (100  $\mu$ g mL<sup>-1</sup>) and varying concentrations of paclitaxel or docetaxel. After incubation at 30 °C for 24–27 h in a humidified chamber, the optical densities were determined using a plate reader at 620 nm.

**Assembly assay:** Freshly cycled tubulin (250 pmol) in 30 mM PEM (30 mM PIPES, 1 mM EGTA, 1 mM MgSO<sub>4</sub>, 0.5 mM GTP, pH 6.9) was assembled in a 50  $\mu$ L volume in the presence of varying concentrations of each taxane for 30 min at 30 °C. Microtubules were collected by sedimentation at 100,000  $\times g$  for 5 min in a Beckman TL-100 ultracentrifuge. The Bradford assay<sup>[10]</sup> was used to determine the protein concentration in the supernatant and in the pellet suspended in 0.1 M NaOH. Data were fitted with the sigmoidal dose response nonlinear curve fitting equation found in Prism 4.03 (Graphpad Software Inc., La Jolla, CA, USA).

**Competition-binding assay:** Freshly cycled tubulin was assembled (250 pmol) in 100 mM PEM (100 mM PIPES, 1 mM EGTA, 1 mM MgSO<sub>4</sub>, 0.5 mM GTP, pH 6.9) in a 50  $\mu$ L volume at 30 °C for 30 min. The preformed microtubules were then incubated in the presence

of a mixture of 5  $\mu$ M <sup>3</sup>H-paclitaxel (420  $\mu$ Ci/ $\mu$ mol) and a varying concentration of unlabelled docetaxel. After 30 min, microtubules were collected by centrifugation and suspended in 0.1 M NaOH. Protein was determined by the Bradford assay<sup>[10]</sup> and <sup>3</sup>H-paclitaxel by scintillation counting. In the absence of docetaxel, incorporation of <sup>3</sup>H-paclitaxel was 0.65 mol per mol tubulin.

**Molecular modeling:** All of the simulations were performed in SYBYL (Version 7.3) with the Tripos force field<sup>[15]</sup> and Gasteiger–Marsili electrostatics<sup>[16]</sup> within a nonbonding threshold of 8.0 Å. Initial structures for the ligand–tubulin complexes were constructed from the tubulin crystal structure (PDB ID 1 JFF).<sup>[17]</sup> Docetaxel complexes were created by hand-editing the native paclitaxel structure. Models for mutants were created by *in silico* mutation within SYBYL Biopolymer toolkit. All other energetic and convergence parameters were left at default values. Interaction enthalpies were determined as the difference between the energy of the complex and the sum of the energies of the isolated ligand and receptor. To allow for relaxation effects specific to each complex, the ligand plus all residues within 8.0 Å of the ligand were permitted to relax for 100 molecular mechanics steps, with the remainder of the tubulin structure held fixed. The position of each ligand was further optimized by allowing it to relax to molecular mechanics convergence with the entire receptor held fixed.

## Acknowledgements

This work was supported by NIH grant CA105305.

**Keywords:** molecular modeling • mutagenesis • taxanes • tubulin • yeast

- [1] F. Mollinedo, C. Gajate, *Apoptosis* **2003**, *8*, 413.
- [2] M. A. Jordan, *Curr. Med. Chem. Anticancer Agents* **2002**, *2*, 1.
- [3] P. B. Schiff, J. Fant, S. B. Horwitz, *Nature* **1979** *277*, 665.
- [4] R. M. Buey, I. Barasoain, E. Jackson, A. Meyer, P. Giannakakou, I. Paterson, S. Mooberry, J. M. Andreu, J. F. Diaz, *Chem. Biol.* **2005**, *12*, 1269.
- [5] M. L. Gupta, Jr., C. J. Bode, G. I. Georg, R. H. Himes, *Proc. Natl. Acad. Sci. USA* **2003**, *100*, 6394.
- [6] J. P. Snyder, J. H. Nettles, B. Cornett, K. H. Downing, E. Nogales, *Proc. Natl. Acad. Sci. USA* **2001**, *98*, 5312.
- [7] A. Decottignies, A. M. Grant, J. W. Nichols, H. de Wet, D. B. McIntosh, A. Goffeau, *J. Biol. Chem.* **1998**, *273*, 12612.
- [8] T. B. Foland, W. L. Dentler, K. A. Suprenant, M. L. Gupta, Jr., R. H. Himes, *Yeast* **2005**, *22*, 971.
- [9] R. A. Entwistle, R. D. Winefield, T. B. Foland, G. H. Lushington, R. H. Himes, *FEBS Lett.* **2008**, *582*, 2467.
- [10] M. M. Bradford, *Anal. Biochem.* **1976**, *72*, 248.
- [11] T. Ganesh, R. C. Guza, S. Bane, R. Ravindra, N. Shanker, A. S. Lakdawala, J. P. Snyder, D. G. I. Kingston, *Proc. Natl. Acad. Sci. USA* **2004**, *101*, 10006.
- [12] D. G. I. Kingston, S. Bane, S. , J. P. Snyder, *Cell Cycle* **2005**, *4*, 279.
- [13] A. A. Alcaraz, A. K. Mehta, S. A. Johnson, J. P. Snyder, *J. Med. Chem.* **2006**, *49*, 2478.
- [14] Y. Paik, C. Yang, B. Metaferia, S. Tang, S. Bane, R. Ravindra, N. Shanker, A. A. Alcaraz, S. A. Johnson, J. Schaefer, R. D. O'Connor, L. Cegelski, J. P. Snyder, D. G. I. Kingston, *J. Am. Chem. Soc.* **2007**, *129*, 361.
- [15] M. Clark, R. D. Cramer III, N. Van Opdenbosch, *J. Comput. Chem.* **1989**, *10*, 982.
- [16] J. Gasteiger, M. Marsili, *Tetrahedron* **1980** *36*, 3219.
- [17] J. Lowe, H. Li, K. H. Downing, E. Nogales, (2001) *J. Mol. Biol.* **2001**, *313*, 1045.

---

Received: September 3, 2008

Published online on November 5, 2008